

Measurement of the coupling constant in a two-frequency VECSEL

V. Pal¹, P. Trofimoff², B.-X. Miranda^{2,4}, G. Baili³, M. Alouini^{3,4},
L. Morvan³, D. Dolfi³, F. Goldfarb², I. Sagnes⁵, R. Ghosh¹,
and F. Bretenaker²

¹*School of Physical Sciences, Jawaharlal Nehru University, New Delhi 110067, India*

²*Laboratoire Aimé Cotton, CNRS-Université Paris Sud 11, Campus d'Orsay, 91405 Orsay Cedex, France*

³*Thales Research & Technology, 1 av. Augustin Fresnel, 91767 Palaiseau Cedex, France*

⁴*Institut de Physique de Rennes, UMR CNRS 6251, Campus de Beaulieu, 35042 Rennes Cedex, France*

⁵*Laboratoire de Photonique et Nanostructures, CNRS, Route de Nozay, 91460 Marcoussis, France*

Fabien.Bretenaker@lac.u-psud.fr

Abstract: We measure the coupling constant between the two perpendicularly polarized eigenstates of a two-frequency Vertical External Cavity Surface Emitting Laser (VECSEL). This measurement is performed for different values of the transverse spatial separation between the two perpendicularly polarized modes. The consequences of these measurements on the two-frequency operation of such class-A semiconductor lasers are discussed.

© 2010 Optical Society of America

OCIS codes: (140.7260) Vertical cavity surface emitting lasers; (140.3460) Lasers; (060.5625) Radio frequency photonics.

References and links

1. G. Pillot, L. Morvan, M. Brunel, F. Bretenaker, D. Dolfi, M. Vallet, J.-P. Huignard, and A. Le Floch, "Dual-frequency laser at 1.5 μm for optical distribution and generation of high-purity microwave signals," *J. Lightwave Technol.* **26**, 2764-2773 (2008).
2. R. Czarny, M. Alouini, C. Larat, M. Krakowski, and D. Dolfi, "THz-dual-frequency $\text{Yb}^{3+}:\text{KGd}(\text{WO}_4)_2$ laser for continuous-wave THz generation through photomixing," *Electron. Lett.* **40**, 942-943 (2004).
3. L. Morvan, N. D. Lai, D. Dolfi, J.-P. Huignard, M. Brunel, F. Bretenaker, and A. Le Floch, "Building blocks for a two-frequency laser lidar-radar: a preliminary study," *Appl. Opt.* **41**, 5702-5712 (2002).
4. K. Otsuka, P. Mandel, S. Bielański, D. Derozier, and P. Glorieux, "Alternate time scales in multimode lasers," *Phys. Rev. A* **46**, 1692-1695 (1992).
5. M. Brunel, A. Amon, and M. Vallet, "Dual-polarization microchip laser at 1.53 μm ," *Opt. Lett.* **30**, 2418-2420 (2005).
6. M. Brunel, F. Bretenaker, S. Blanc, V. Crozatier, J. Brisset, T. Merlet, and A. Poezevara, "High-spectral purity RF beat note generated by a two-frequency solid-state laser in a dual thermo-optic and electro-optic phase-locked loop," *IEEE Photon. Tech. Lett.* **16**, 870-872 (2004).
7. L. Morvan, D. Dolfi, J.-P. Huignard, S. Blanc, M. Brunel, M. Vallet, F. Bretenaker, and A. Le Floch, "Dual-frequency laser at 1.53 μm for generating high-purity optically carried microwave signals up to 20 GHz," in *Conference on Lasers and Electro-Optics/International Quantum Electronics Conference and Photonic Applications Systems Technologies*, Technical Digest (CD) (Optical Society of America, 2004), paper CTuL5.

8. G. Baili, M. Alouini, D. Dolfi, F. Bretenaker, I. Sagnes, and A. Garnache, "Shot-noise limited operation of a monomode high cavity finesse semiconductor laser for microwave photonics applications," *Opt. Lett.* **32**, 650-652 (2007).
9. G. Baili, F. Bretenaker, M. Alouini, D. Dolfi, and I. Sagnes, "Experimental investigation and analytical modeling of excess intensity noise in semiconductor class-A lasers," *J. Lightwave Tech.* **26**, 952-961 (2008).
10. G. Baili, L. Morvan, M. Alouini, D. Dolfi, F. Bretenaker, I. Sagnes, and A. Garnache, "Experimental demonstration of a tunable dual-frequency semiconductor laser free of relaxation-oscillations," *Opt. Lett.* **34**, 3421-3423 (2009).
11. M. Sargent III, M. O. Scully, and W. E. Lamb, Jr., *Laser Physics* (Addison-Wesley, 1974).
12. M. M.-Tehrani and L. Mandel, "Coherence theory of the ring laser," *Phys. Rev. A* **17**, 677-693 (1978).
13. A. Laurain, M. Myara, G. Beaudoin, I. Sagnes, and A. Garnache, "High power single-frequency continuously-tunable compact extended-cavity semiconductor laser," *Opt. Expr.* **17**, 9503-9508 (2009).
14. A. E. Siegman, *Lasers* (University Science Books, 1986), pp. 992-999.
15. M. Brunel, M. Vallet, A. Le Floch, and F. Bretenaker, "Differential measurement of the coupling constant between laser eigenstates," *Appl. Phys. Lett.* **70**, 2070-2072 (1997).
16. M. Alouini, F. Bretenaker, M. Brunel, A. Le Floch, M. Vallet, and P. Thony, "Existence of two coupling constants in microchip lasers," *Opt. Lett.* **25**, 896-898 (2000).
17. A. McKay, J. M. Dawes, and J.-D. Park, "Polarisation-mode coupling in (100)-cut Nd:YAG," *Opt. Expr.* **15**, 16342-16347 (2007).
18. S. Schwartz, G. Feugnet, M. Rebut, F. Bretenaker, and J.-P. Pocholle, "Orientation of Nd³⁺ dipoles in yttrium aluminum garnet: Experiment and model," *Phys. Rev. A* **79**, 063814 (2009).
19. J. Talghader and J. S. Smith, "Thermal dependence of the refractive index of GaAs and AlAs measured using semiconductor multilayer optical cavities," *Appl. Phys. Lett.* **66**, 335-337 (1995).
20. M. San Miguel, Q. Feng, and J. V. Moloney, "Light-polarization dynamics in surface-emitting semiconductor lasers," *Phys. Rev. A* **52**, 1728-1739 (1995).
21. M. P. van Exter, R. F. M. Hendriks, and J. P. Woerdman, "Physical insight into the polarization dynamics of semiconductor vertical-cavity lasers," *Phys. Rev. A* **57**, 2080-2090 (1998).
22. D. Burak, J. V. Moloney, and R. Binder, "Microscopic theory of polarization properties of optically anisotropic vertical-cavity surface-emitting lasers," *Phys. Rev. A* **61**, 053809 (2000).

1. Introduction

Two-frequency lasers have proved to be interesting sources for the optical distribution and generation of radar local oscillators [1], the optical generation of high spectral purity CW THz radiation [2], or for pulsed or CW lidar-radar systems [3]. In all these examples of use, the two-frequency lasers were based on solid-state active medium, such as Er-Yb doped glasses or Nd doped crystals. Due to the long lifetime of the upper level population, typically in the 100 μ s to 10 ms range, these lasers are the so-called class-B lasers, i. e., their photon lifetime is much shorter than the population inversion lifetime. This means that these lasers exhibit relaxation oscillations. In the case of a two-oscillating-mode laser, there are two relaxation oscillation frequencies, corresponding respectively to the in-phase and the antiphase oscillation of the intensities of the two modes [4]. The presence of these resonances leads to a strong intensity noise in the kHz to MHz frequency domain [5] which constitutes the actual limitation of the noise of these lasers when they are used to generate low noise microwave signals [6, 7]. However, it has recently been shown that Vertical External Cavity Surface Emitting Lasers (VECSELs) can belong to the class-A dynamical regime and exhibit a very low intensity noise [8, 9]. This is why we recently investigated the possibility to reach two-frequency oscillation in a VECSEL [10]. However, the simultaneous oscillation of the two modes of the laser relies on the value of the nonlinear coupling constant C between these modes [11]. In order to decrease C well below the critical value of 1, we implemented a spatial separation of the two polarization modes in the active medium [10]. Then, it seems important in the present context to control the value of C in order to reach a stable two-frequency regime for a minimum spatial separation of the two modes. Indeed, a very large spatial separation would allow differential noises to appear, thus increasing the beat frequency jitter. Moreover, it is well known that the value of C plays an important role in the noise correlations between the two modes in class-A lasers [12]. The aim

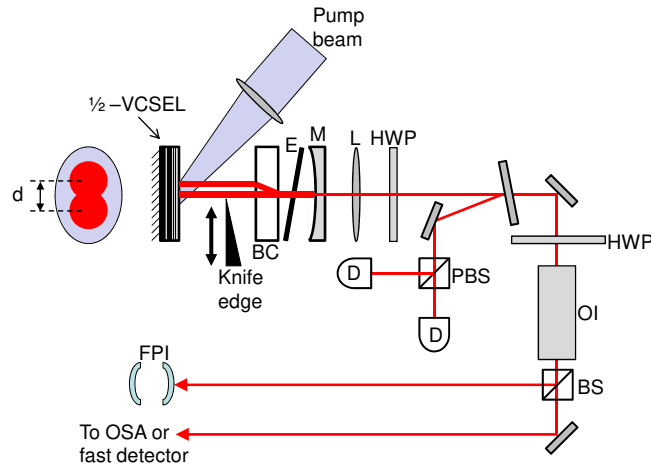


Fig. 1. Experimental setup. BC: birefringent crystal; HWP: half-wave plate; M: cavity mirror; E: étalon; FPI: Fabry-Perot interferometer. PBS: polarization beam-splitter; BS: beam splitter; L: lens; D: detector; OI: optical isolator; OSA: optical spectrum analyzer.

of the present work is consequently to measure the value of C in a two-frequency VECSEL for different values of the spatial separation of the two orthogonally polarized modes, as a first step in optimizing this kind of lasers.

2. Description of the experiment

The experimental setup is schematized in Fig. 1. The laser is based on a 1/2-VCSEL grown by Metal Organic Chemical Vapor Deposition (MOCVD) [13] consisting in a 27.5-period GaAs/AlAs Bragg mirror (99.9% reflectivity). Gain at $1 \mu\text{m}$ is provided by six strained balanced InGaAs/GaAsP quantum wells covered by an anti-reflection coating. The structure is bonded to a SiC substrate and maintained at 20°C thanks to a Peltier thermo-electric cooler. The pump system consists in a 808 nm pigtailed diode laser delivering up to 3 W and focused on the gain chip to a $100 \mu\text{m}$ diameter spot with an incidence angle of about 30° . The cavity is closed with a 50 mm radius of curvature concave mirror reflecting 99% of the intensity. The cavity length is about 47 mm. In these conditions, the photon lifetime is of the order of 15 ns, which is much longer than the carrier lifetime (which is of the order of 3 ns), thus ensuring class-A dynamical behavior for the laser [8]. In these conditions, the laser threshold corresponds to a pump power of about 270 mW.

Dual-polarization oscillation is achieved by introducing a birefringent YVO_4 crystal (BC) inside the cavity. This crystal, which is anti-reflection coated at $1 \mu\text{m}$, introduces a polarization walk-off d proportional to its thickness. We have three different crystals of thicknesses 1, 0.5, and 0.2 mm, corresponding to $d = 100, 50,$ and $20 \mu\text{m}$, respectively. When the horizontal position of the pump spot is carefully adjusted to provide as much pump power to the two spatially separated beams, one can achieve the simultaneous oscillation of the two perpendicularly linearly polarized beams which correspond to the ordinary and extraordinary polarizations of BC and are separated by d in the active structure. Perfect spatial overlapping of the beams between the crystal BC and the cavity mirror M is ensured by the fact that M is concave while the Bragg mirror is plane. To make each polarization oscillate at a single frequency, a $150\text{-}\mu\text{m}$ thick uncoated glass étalon is introduced inside the cavity. The orientation of the étalon is adjusted to make the two cross-polarized modes oscillate in the same longitudinal mode of the cavity, as checked using an optical spectrum analyzer. The frequency difference between the two polar-

izations, which is thus smaller than the 3.2 GHz free spectral range (FSR) of the cavity, can then be measured using either a 10 GHz FSR Fabry-Perot interferometer or a fast photodiode followed by an electrical spectrum analyzer. We also use these apparatus to make sure that no high-order transverse mode is oscillating. The powers of the two polarizations can be equalized by adjusting the horizontal position of the pump beam. In these conditions, with the 200 μm -thick crystal for example, the laser threshold increases up to 1.1 W. An output power of 220 mW with a stable dual-frequency behavior is obtained with a pump power of 2600 mW. For higher pump powers, the dual-frequency behavior of the laser is no longer stable.

3. Principle of the measurement

In a class-A laser, the intensities I_o and I_e of the two ordinary- and extraordinary-polarized modes obey the following differential Eqs. [14]:

$$\frac{dI_o}{dt} = \frac{I_o}{\tau_o} \left[-1 + \frac{r_o}{1 + (I_o + \xi_{oe}I_e)/I_{\text{sat}}} \right], \quad (1)$$

$$\frac{dI_e}{dt} = \frac{I_e}{\tau_e} \left[-1 + \frac{r_e}{1 + (I_e + \xi_{eo}I_o)/I_{\text{sat}}} \right], \quad (2)$$

where τ_o and τ_e are the lifetimes of the ordinary and extraordinary polarized photons, r_o and r_e are the excitation ratios of the two modes (ratio of the unsaturated gain to the losses), I_{sat} is the saturation intensity of the active medium, and ξ_{oe} and ξ_{eo} are the ratios of the cross- to self-saturation coefficients for the two modes.

The steady-state solution of Eqs. (1) and (2) corresponding to the simultaneous oscillation of the two modes is given by:

$$I_o = I_{\text{sat}} \frac{(r_o - 1) - \xi_{oe}(r_e - 1)}{1 - C}, \quad (3)$$

$$I_e = I_{\text{sat}} \frac{(r_e - 1) - \xi_{eo}(r_o - 1)}{1 - C}, \quad (4)$$

where

$$C = \xi_{oe}\xi_{eo} \quad (5)$$

is the nonlinear coupling constant, as defined by Lamb [11]. The solution given by Eqs. (3) and (4) may be stable only if $C < 1$ [11]. Different methods have been used to measure C [15, 16, 17]. Here, we choose to observe the response of the intensities of the two modes to the introduction of extra losses for only one of these modes. From Eqs. (3) and (4), we can see that the values of ξ_{oe} and ξ_{eo} can be deduced from the observation of the response of the mode intensities to a modification of the losses and/or of the gain of the modes:

$$\xi_{eo} = -\frac{\partial I_e / \partial r_o}{\partial I_o / \partial r_o}, \quad (6)$$

$$\xi_{oe} = -\frac{\partial I_o / \partial r_e}{\partial I_e / \partial r_e}. \quad (7)$$

Thus, by modulating the losses of the ordinary mode and by measuring the modulation amplitudes of the intensities of the two modes, we can use Eq. (6) to determine ξ_{eo} . The same procedure can be performed using Eq. (7) to measure ξ_{oe} by modulating the losses of the extraordinary mode.

4. Results and discussion

In our experiment, we perform this modulation of the losses experienced by one mode only by using a knife-edge introduced in the part of the cavity in which the two modes are spatially separated (see Fig. 1). This knife-edge is mounted on a piezo-electric transducer in order to modulate the amount of diffraction losses introduced. The truncation losses introduced by the knife-edge are much smaller than 1 %, allowing us to neglect any modification of the spatial profile of the beam.

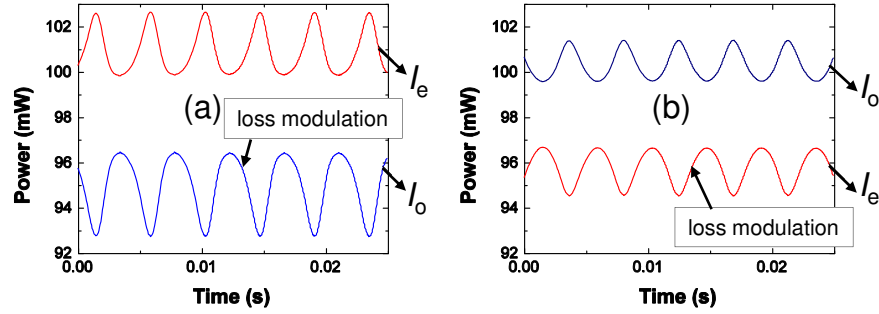


Fig. 2. Experimental results for a spatial separation $d = 20 \mu\text{m}$. (a) Evolution of the powers of the ordinary and extraordinary modes when the losses of the ordinary mode are modulated at 227 Hz. (b) Same as (a) when the losses of the extraordinary mode are modulated.

Figure 2 reproduces typical experimental traces obtained by this method. In this example, the separation between the ordinary and extraordinary modes is $d = 20 \mu\text{m}$. Without the knife-edge, the laser threshold corresponds to a pump power of 1.14 W. The introduction of the knife-edge inside one of the beams increases this threshold by about 50 mW. This Fig. was obtained with a pump power of 2.21 W. The output powers of the two modes are about 100 mW. To obtain the results of Fig. 2, the position of the knife-edge is modulated at 227 Hz. These results show that, as expected from Eqs. (6) and (7), the modulations of the intensities of the two modes are in antiphase. The modulation of the losses is slow enough compared to the time constants of the system, namely the photon lifetime in the cavity and the carrier lifetime, to allow us to consider that the steady-state analysis of section 3 is valid. Then, using Eqs. (6) and (7), the results of Figs. 2(a) and 2(b) lead to $\xi_{eo} = 0.76$ and $\xi_{oe} = 0.85$, respectively. This leads to the following value of the coupling constant in this case:

$$C_{d=20 \mu\text{m}} = \xi_{oe}\xi_{eo} = 0.64 . \quad (8)$$

We have checked experimentally that the value of C is independent of the pump power and of the amount of losses introduced by the knife-edge. The values of ξ_{eo} and ξ_{oe} slightly vary from one measurement to the other, as already observed in the case of Er,Yb doped glass [16] and Nd:YAG [18], but their product C remains constant to ± 0.05 . We then performed the same measurement for a larger spatial separation $d = 50 \mu\text{m}$ (see Fig. 3). These measurements were performed in conditions similar to the ones of Fig. 2. By comparing Fig. 3 with Fig. 2, one can clearly see that the intensity of the mode whose losses are not modulated is less affected by the modulation of the losses of the other modes, illustrating the decrease in the coupling allowed by the increase of the spatial separation d . By using again Eqs. (6) and (7), the curves of Figs. 3(a) and 3(b) lead to $\xi_{eo} = 0.34$ and $\xi_{oe} = 0.53$, respectively. Their product leads to:

$$C_{d=50 \mu\text{m}} = \xi_{oe}\xi_{eo} = 0.18 . \quad (9)$$

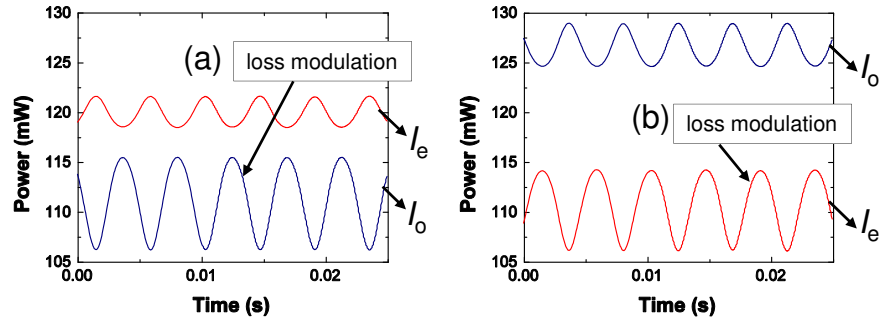


Fig. 3. Same as Fig. 2 for $d = 50 \mu\text{m}$.

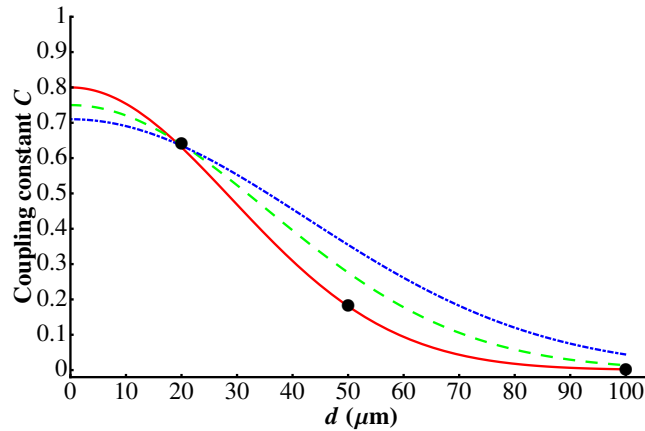


Fig. 4. Evolution of the coupling constant C versus spatial separation d . The filled circles are the measurements and the full lines are given by Eq. (12) with $C_0 = 0.8$ and $w_0 = 41 \mu\text{m}$ (full red line), $C_0 = 0.75$ and $w_0 = 50 \mu\text{m}$ (dashed green line), and $C_0 = 0.71$ and $w_0 = 60 \mu\text{m}$ (dot-dashed blue line)

We eventually used the 1-mm long birefringent crystal which introduces a transverse spatial separation $d = 100 \mu\text{m}$ between the ordinary and extraordinary modes. With this crystal, we could detect absolutely no variation of the intensity of one mode when the losses of the other mode are modulated. We thus conclude that:

$$C_{d=100 \mu\text{m}} \approx 0. \quad (10)$$

These measurements are indicated as filled circles in Fig. 4. In principle, the coupling constant should evolve like the overlap integral of the two modes in the active medium, namely

$$C = C_0 \frac{\int I_1(x,y)I_2(x,y)dxdy}{(\int I_1^2(x,y)dxdy \int I_2^2(x,y)dxdy)^{1/2}}, \quad (11)$$

where C_0 is the coupling constant for superimposed modes, and $I_1(x,y)$ and $I_2(x,y)$ are the mode intensity profiles in the active medium. By taking two Gaussian profiles of equal radii w_0 separated by a distance d , Eq. (11) becomes:

$$C = C_0 e^{-d^2/w_0^2}. \quad (12)$$

To compare Eq. (12) with experiments, we tried to determine w_0 by two means. The first method consists in carefully measuring the cavity length by measuring the beat note frequency between two successive longitudinal modes when the laser is multimode. We then obtain a cavity optical length $L = 4.73$ cm. Since the thicknesses of the 1/2-VCSEL, the étalon, and the birefringent crystal are very small compared with the cavity length, we use this value as the cavity geometrical length to compute the size of the waist for a simple planar-concave cavity. This leads to $w_0 = 60$ μm . We then adjust the value of C_0 to 0.71 in order to find the correct value of C for $d = 20$ μm . This leads to the dot-dashed blue line in Fig. 4, which provides only a poor agreement with the measurements for $d = 50$ μm and $d = 100$ μm . We then tried to determine w_0 by measuring the divergence of the beam at the output of the laser. Then by taking into account the divergent lens effect due to the traversal of the output mirror, we can deduce the divergence of the intracavity beam and then, finally, the value of w_0 . With that method, we find $w_0 = 50$ μm . By adjusting the value of C_0 to 0.75, we then obtain the dashed green line in Fig. 4. The agreement with measurements is better than before but is still not perfect. A perfect agreement can be obtained for $w_0 = 41$ μm and $C_0 = 0.8$, as evidenced by the full red line in Fig. 4. The reasons why the agreement cannot be better with the two other curves is that i) Eq. (12) leads to a very fast variation of C with w_0 , and ii) our methods to determine w_0 lack precision. In particular, the first one which supposes that our cavity is a planar-concave resonator is not true because the thermal lens induced by the pump in the active medium is strong, preventing the structure from behaving as a simple planar mirror. However, since the thermo-optic coefficients of GaAs and AlAs are positive [19], we expect the thermal lens effect to be positive, which should lead, for our cavity configuration, to an increase of the mode radius inside the structure instead of the observed decrease. This point thus requires further investigations.

One potentially important conclusion of the present work is that the high value of C_0 (of the order of 0.8) explains why it is so difficult to obtain robust oscillation of the two modes without performing a spatial separation. However, since C_0 is smaller than 1, the simultaneous oscillation of the two modes is in principle possible even in the absence of spatial separation. However, it requires a careful balance of the losses and gains of the two modes to force them to oscillate simultaneously.

5. Conclusion

In conclusion, we have measured the coupling constant for the two perpendicularly polarized modes of a laser based on strained balanced InGaAs/GaAsP quantum wells. The values of the coupling constant that we obtained are useful for the design of relaxation-oscillation-free two-frequency lasers [10]. In particular, it is found that the simultaneous oscillation of two perpendicularly polarized modes is in principle possible without spatially separating them in the active medium. In the future, we plan to gain better understanding of the values we get for this coupling constant using either models based on the introduction of carrier spin dynamics [20, 21] or on a more complete microscopic theory of the anisotropy of gain saturation in such quantum wells [22]. This should help us to optimize these lasers and, in particular, reduce their noise.

Acknowledgments

The authors acknowledge partial support from the “Agence Nationale de la Recherche” (projects 2POLEV and NATIF), the “Triangle de la Physique”, and the Indo-French Centre for the Promotion of Advanced Research. One of the authors (VP) thanks the Council of Scientific and Industrial Research, India, for financial support.